Gabor deconvolution of seismic data for source waveform and Q correction

Gary F. Margrave, Michael P. Lamoureux, Jeff P. Grossman, and Victor Iliescu, The University of Calgary*

Summary

We present a novel approach to nonstationary seismic deconvolution using the Gabor transform. This nonstationary transform represents a signal as a superposition of sinusoids that are localized by time-shifted windows. The resulting time-frequency decomposition is a suite of local Fourier transforms that facilitates nonstationary spectral analysis or filtering. In a result that generalizes the seismic convolutional model, we show that the Gabor transform of a nonstationary seismic signal is the product of source signature, Q filter, and reflectivity effects. We use this spectral factorization theorem as a basis for a new deconvolution algorithm in the Gabor domain. We estimate the Gabor spectrum of the underlying reflectivity directly from the Gabor spectrum of an attenuated seismic signal. Tests on synthetic and real data show that our method works well and combines the effects of source-signature inversion and a data-driven inverse Q filter. In comparison with a stationary Wiener deconvolution, our Gabor deconvolution is similar within the Wiener design gate and superior elsewhere.

Introduction

In 1946, Dennis Gabor, the inventor of the hologram, proposed the expansion of a wave in terms of *Gaussian wave packets* (e.g. a sine wave multiplied by a Gaussian function). Multiplying a signal by a specific Gaussian window and Fourier transforming gives a local Fourier spectrum. Clearly such a spectrum is not unique since the width of the Gaussian is arbitrary; but nevertheless, it is extremely useful. If this process is iterated for a suite of window positions, the result is a time-frequency decomposition called a Gabor transform. Furthermore, for any reasonable choice of window (e.g., a Gaussian or any continuous function on a finite, closed interval), the inverse transform is possible, and a nonstationary filter can be achieved by modifying the decomposition before reconstruction.

We present the theory of the continuous Gabor transform and a discrete Gabor transform based on a partition of unity. The modern theory of the discrete Gabor transform is usually attributed to Bastiaans (1980). A complete overview is found in Feichtinger and Strohmer (1998). We apply the continuous Gabor transform to a mathematical model of a nonstationary seismogram to show that the Gabor spectrum factors into wavelet, Q filter, and reflectivity components. This result was postulated previously by Scheopp and Margrave (1998). We use this spectral factorization theorem to develop a Gabor deconvolution algorithm that is a direct extension of standard (e.g. Wiener) methods to the nonstationary case. The resulting minimum-phase deconvolution technique simultaneously accomplishes the tasks of source waveform inversion and (apparent) inverse Q filtering.

The Gabor transform

Following Mertins (1999), we define the continuous Gabor transform of a signal s(t) as

$$V_g s(\tau, f) = \int_{-\infty}^{\infty} s(t)\, g(t-\tau)\, e^{-2\pi i f t} dt \qquad (1)$$

where $g(t)$ is the *Gabor analysis window* and τ is the location of the window center. Although we use $g(t)$ as a Gaussian function, the theory works well for quite general windows. The signal is recovered with the *inverse Gabor transform*

$$s(t) = \int_{-\infty}^{\infty}\int_{-\infty}^{\infty} V_g s(\tau, f)\, \gamma(t-\tau)\, e^{2\pi i f t} df d\tau \qquad (2)$$

where $\gamma(t)$ is the *Gabor synthesis window*. The analysis and synthesis windows must satisfy the condition

$$\int_{-\infty}^{\infty} g(t)\gamma(t)\, dt = 1 . \qquad (3)$$

Given equation (1) and the condition (3), the derivation of equation (2) is straightforward and can be found in Mertins (1999).

Though the discrete Gabor transform can be formulated for very general time-frequency lattices (e.g. Feichtinger and Strohmer 1998), we choose a simpler approach because the more general approach can be computationally slow. Unlike the discrete Fourier transform that expands a signal into an orthonormal basis, the discrete Gabor transform expands into a more general construct called a *frame*. By choosing windows that form a *partition of unity*, a simple Gabor frame, called a *tight* frame, can be implemented (Grochenig, 2001, p118). Furthermore, most of the calculations can be done with an FFT so that numerical efficiency is fairly good. Let $w(t)$ be a set of windows satisfying the property

$$\sum_{k\in\mathbb{Z}} w(t-k\Delta\tau) \equiv \sum_{k\in\mathbb{Z}} w_k(t) = 1 \qquad (4)$$

and let $g_k(t) = w_k(t)^p$ and $\gamma_k(t) = w_k(t)^q$ with $p+q=1$. Then we define the forward discrete Gabor transform as

$$\hat{s}_k(f) = F\left[s_k(\cdot)\right](f); \qquad s_k(t) \equiv s(t)\, g_k(t) \qquad (5).$$

where *F* is the (discrete) Fourier transform. We use the "hat" notation for the *Fourier* transform. Here notation shows the Gabor transform of $s(t)$ is the Fourier transform of the *Gabor slice* $s_k(t)$. (For simplicity, we use a continuous notation for signal, window, and Fourier transform and a discrete index for window position. For fully discrete formulae, the normal notation for discrete signals is easily employed.) The signal is recovered by the inverse discrete Gabor transform given by

$$s(t) = \sum_{k\in\mathbb{Z}} \gamma_k(t)\, F^{-1}\left[\hat{s}_k(\cdot)\right](t) . \qquad (6)$$

Substitution of equation (5) into (6) shows that the signal is recovered exactly due to the property of equation (4) and $p+q=1$.

Gabor deconvolution

In this work we take $p=1$ and $q=0$ and choose the set $\{w_k(t)\}$ to be Gaussian windows such that

$$\sum_{k\in\mathbb{Z}} w_k(t) \approx 1 \qquad (7)$$

where

$$w_k(t) = \frac{\Delta\tau}{T\sqrt{\pi}} e^{-[t-k\Delta\tau]^2/T} \qquad (8)$$

with T being the Gaussian (half) width. This approximate partition of unity differs from 1 by an error term, dominated by $\exp(-[\pi T/\Delta\tau]^2)$ that can be made arbitrarily small by increasing the ratio $T/\Delta\tau$. For example, the maximum error is -150 decibels for $T/\Delta\tau = 1.5$ and is negligible for most practical purposes.

Gabor factorization of a nonstationary trace model

We now present a trace model that includes the source signature and the nonstationary effects of dissipation as predicted by the constant-Q model though it does not explicitly model multiples or stratigraphic filtering. The effect of constant Q can be modeled as

$$s_Q(t) = \int_{-\infty}^{\infty}\int_{-\infty}^{\infty} \alpha_Q(\tau, f) r(\tau) e^{2\pi i f[t-\tau]} d\tau df \qquad (9)$$

where $r(\tau)$ is the reflectivity sequence and the constant-Q transfer function is

$$\alpha_Q(\tau, f) = e^{-\pi f\tau/Q + iH(\pi f\tau/Q)} \qquad (10)$$

where H denotes the Hilbert transform over f at constant τ. Equation (9) can be understood as a nonstationary convolution in the sense defined by Margrave (1998).

As defined by equation (9), s_Q models dissipation for an impulsive source. We apply a more general source signature with a stationary convolution and write our final nonstationary trace model as

$$\hat{s}(f) = \hat{w}(f)\int_{-\infty}^{\infty} \alpha_Q(\tau, f) r(\tau) e^{-2\pi i f\tau} d\tau \qquad (11)$$

where $\hat{w}$ and $\hat{s}$ are the Fourier transforms of the source signature and the nonstationary seismic trace respectively. Equation (11) is a replacement for the familiar stationary convolution model.

We have derived an asymptotic result for the continuous Gabor transform of $s(t)$, whose Fourier transform is given by equation (11), as

$$V_g s(\tau, f) \approx \hat{w}(f)\alpha_Q(\tau, f) V_g r(\tau, f) \qquad (12)$$

where the $\approx$ sign means that this is the leading term in an asymptotic series. (Space does not permit us to include our derivation here but we will provide the details upon request.) In words, the continuous Gabor transform of our nonstationary trace is approximately equal to the product of the Fourier transform of the source signature, the constant Q transfer function, and the continuous Gabor transform of the reflectivity. Since, for fixed τ, the Gabor transform is just a Fourier transform, this is a *temporally local* convolutional model. It is a reasonable expectation that a similar relation holds for the discrete Gabor transform.

Figure 1 shows the magnitude of the Gabor transform of a synthetic attenuated signal (the bottom signal of Figure 6). The input signal was computed with equation (11) using a minimum-phase source signature with a dominant frequency of 20 Hz and a Q of 25. The Gabor analysis window used $T = 0.1$ s and $\Delta\tau = 0.01$ s. In Figure 2 is the Gabor magnitude spectrum of the random reflectivity series used to generate the synthetic signal. When the reflectivity spectrum of Figure 4 is multiplied by the constant-Q attenuation surface, $|\alpha_Q(\tau, f)|$, and by $|\hat{w}(f)|$ the result is a very close approximation to the spectrum shown in Figure 2.

A Gabor deconvolution algorithm

Our method of deconvolution estimates the Gabor transform of the reflectivity from the Gabor transform of a nonstationary seismic trace. From equation (12), we divide the Gabor spectrum of the seismic trace by estimates of the source waveform and the Q transfer function. As with stationary deconvolution, this is a nonunique *spectral factorization* problem requiring assumptions about the three spectral components. We assume that $|V_g r(\tau, f)|$ is a rapidly varying function in both variables (Figure 2) while $|\hat{w}(f)|$ is assumed to be independent of τ while smoothly varying in f, and $|\alpha_Q(\tau, f)|$ is an exponential decay surface in both variables.

The simplest Gabor deconvolution algorithm estimates $|\hat{w}(f)||\alpha_Q(\tau, f)|$ by convolving $|V_g s(\tau, f)|$ with a smoother such as a 2D boxcar or other compact function. Often this is a good estimate though results are dependent upon the dimensions of the smoother. However, the smoothing approach gives a biased estimate of $|\hat{w}(f)||\alpha_Q(\tau, f)|$. For example, if $|V_g r(\tau, f)|$ is unity so that $|V_g s(\tau, f)|$ is already equal to $|\hat{w}(f)||\alpha_Q(\tau, f)|$, then the smoother will alter the function and we obtain the wrong answer.

Other spectral factorization methods are possible. Grossman et al. (2002) model a measured Gabor spectrum by least squares using equation (12) and obtain estimates of Q and $|\hat{w}(f)|$. Iliescu and Margrave (2002) compare 2D boxcar smoothing to smoothing along curves of $\tau f = \text{constant}$. If $|\sigma(\tau, f)|$ is a smooth approximation to $|V_g s(\tau, f)|$ that estimates $|\hat{w}(f)||\alpha_Q(\tau, f)|$, then its minimum-phase function is

$$\varphi(\tau, f) = \int_{-\infty}^{\infty} \frac{\ln|\sigma(\tau, f')|}{f - f'} df' \qquad (13)$$

where we assume that $|\sigma(\tau, f)|$ has been designed to have no zeros. Equation (13) is a Hilbert transform over frequency at constant time. Given $|\sigma(\tau, f)|$ and the phase from equation (13), we calculate $\sigma(\tau, f)$ and estimate the Gabor spectrum of the reflectivity as

$$V_g r(\tau, f)_{est} = \frac{V_g s(\tau, f)}{\sigma(\tau, f)}. \qquad (14)$$

Examples

Figure 3 shows a smoothed version of Figure 1 that estimates $|\hat{w}(f)||\alpha_Q(\tau, f)|$. Smoothing in f was accomplished by a Burg spectral estimate (Claerbout, 1976) corresponding to the Fourier estimate in Figure 2. Smoothing in τ was done by convolution with a boxcar of length 0.1 seconds. Dividing the

spectrum of Figure 1 by that of Figure 3 and applying a stationary filter to reject frequencies above 125 Hz gives the estimate of the Gabor spectrum of the reflectivity shown in Figure 4. Comparison with Figure 2 shows that the estimate is quite good. Figure 5 shows the Gabor spectrum of the attenuated signal after AGC and Wiener deconvolution. The Wiener design gate was from 0.35 to 0.65 seconds. This shows the familiar behavior that the Wiener operator over whitens data at earlier times.

Figure 6 summarizes results in the time domain. The Gabor deconvolution matches the bandlimited reflectivity very well and has a much whiter and more stationary appearance than the AGC+Wiener result. The Fourier amplitude spectra of these traces are shown in Figure 7. There is a good correlation between the Gabor result and bandlimited reflectivity spectra while the Weiner result is less similar.

Figures 8 and 9 compare Gabor deconvolution with conventional Wiener deconvolution on a real seismic shot record. The Wiener design gate was from 1.0 to 1.6 seconds and within this zone the results are superficially similar. However, a detailed inspection shows phase and amplitude differences and a different response to ground roll. Also apparent is that the Wiener result is dramatically inferior to Gabor above the design gate.

Conclusions

We have described the Gabor transform in both continuous and discrete forms. Using a simplified nonstationary trace model, we derived a spectral factorization in the Gabor domain, the basis for our deconvolution procedure. Our Gabor deconvolution estimates the propagating wavelet spectrum by smoothing the magnitude of the Gabor spectrum of the seismic trace. Phase is calculated by a minimum-phase assumption. Reflectivity is estimated by dividing the Gabor spectrum of the seismic trace by an estimate of the propagating wavelet. Our examples show that this new technique usually gives better results than Wiener deconvolution.

Acknowledgements

We are grateful to our sponsors: NSERC (Natural Sciences and Engineering Research Council), MITACS (Mathematics of Information Technology and Complex Systems), PIMS (Pacific Institute for the Mathematical Sciences), Imperial Oil, and CREWES (Consortium for Research in Elastic Wave Exploration Seismology).

References

Bastiaans, M. J., 1980, Gabor's expansion of a signal into Gaussian elementary signals: Proceedings of the IEEE, **68**, 538-539.

Claerbout, J. F., 1976, Fundamentals of Geophysical Data Processing: McGraw-Hill.

Feichtinger, H. G., and Strohmer, T., 1998, Gabor analysis and algorithms: Theory and applications: Birkhauser, ISBN 0-8176-3959-4.

Gabor, D., 1946, Theory of communication: J. IEEE (London), **93(III)**, 429-457.

Grochenig, K., 2001, Foundations of time-frequency analysis: Brikhauser, ISBN 0-8176-4022-3.

Grossman, J. P., Margrave, G. F., Lamoureux, M. P., and Aggarwala, R., 2002, Constant-Q wavelet estimation via a Gabor spectral model: CSEG Convention Expanded Abstracts.

Iliescu, V., and Margrave, G. F., 2002, Reflectivity amplitude restoration in Gabor deconvolution: CSEG Convention Expanded Abstracts.

Margrave, G. F., 1998, Theory of nonstationary linear filtering in the Fourier domain with application to time-variant filtering: Geophysics, **63**, 244-259.

Mertins, A., 1999, Signal Analysis: John Wiley and Sons, ISBN 0-471-98626-7.

Schoepp, A. R., and Margrave, G. F., 1998, Improving seismic resolution with nonstationary deconvolution: 68th Annual SEG meeting, New Orleans, La.

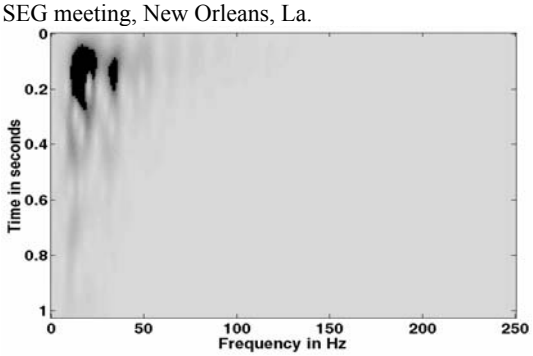

Figure 1. The Gabor (magnitude) spectrum of the attenuated signal of Figure 6. Darker shading indicates greater values.

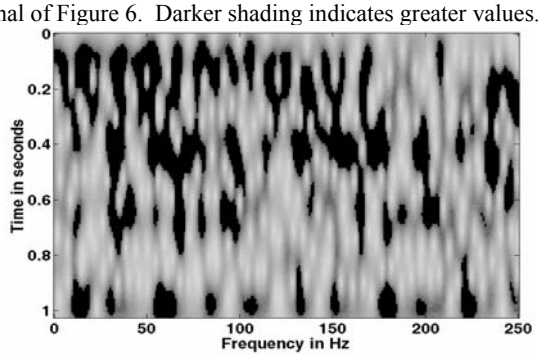

Figure 2. The Gabor (magnitude) spectrum of the reflectivity used to make the attenuated signal of Figure 1.

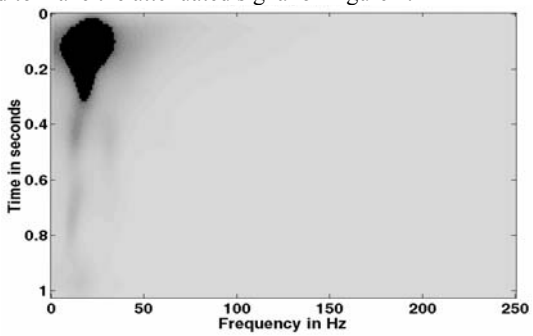

Figure 3. The smoothed Gabor (Burg) spectrum corresponding to Figure 1.

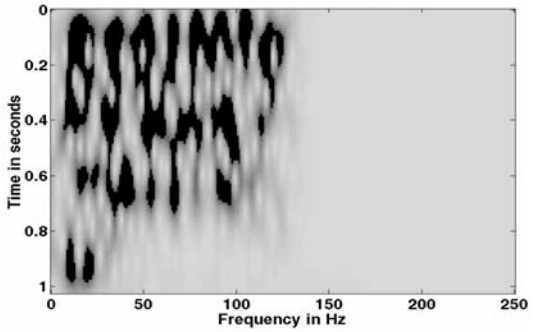

Figure 4. The result of dividing the Gabor spectrum in Figure 1 by that in Figure 3. This is the estimate of the Gabor spectrum of the reflectivity. Compare with Figure 2. A stationary highcut filter has been applied to reject frequencies above 125 Hz.

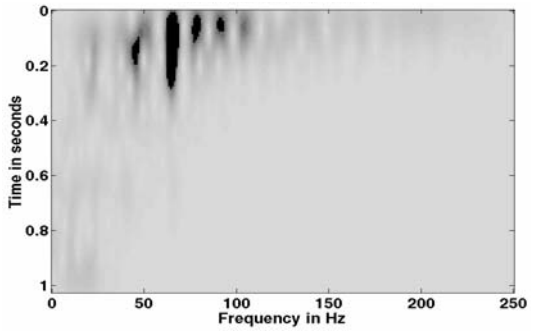

Figure 5. The Gabor spectrum of the result of performing AGC followed by Wiener deconvolution of the attenuated signal of Figure 6. This is the Gabor spectrum of the trace (after AGC+Wiener) shown in Figure 6.

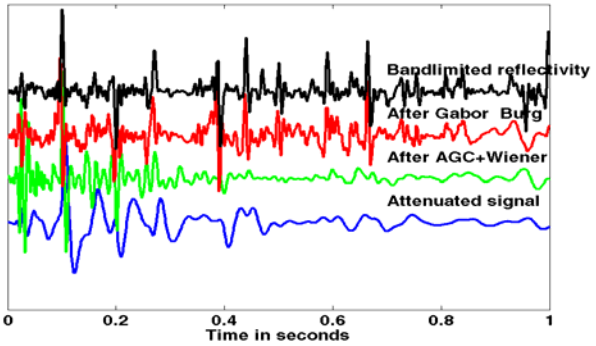

Figure 6. The attenuated signal is shown (bottom) compared with a conventional AGC→Wiener deconvolution (second) and a Gabor/Burg deconvolution (third) and finally a bandlimited reflectivity (top). The reflectivity and the Gabor deconvolution have been bandlimited to less than 125 Hz.

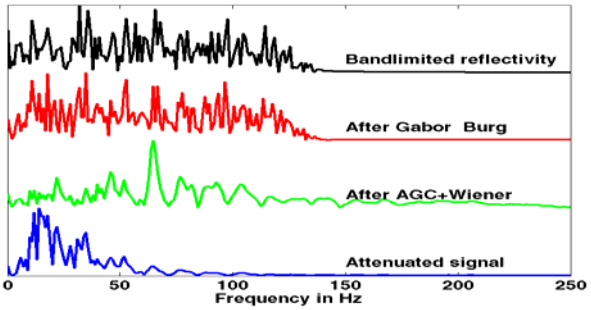

Figure 7. The Fourier spectra (entire trace) of the signals in Figure 6.

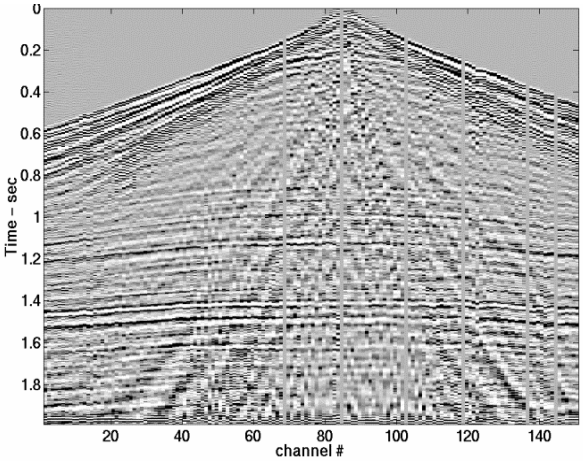

Figure 8. A seismic shot record processed with Gabor deconvolution

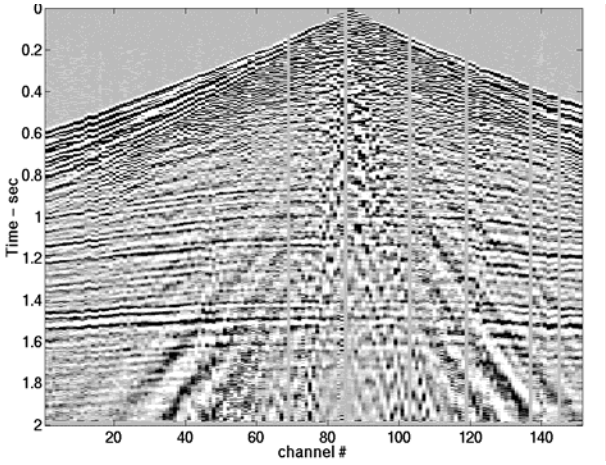

Figure 9. The same seismic shot record as Figure 8 processed with exponential gain and Wiener deconvolution.